Plasma Science and Technology

PAPER

Bended probe diagnostics of the plasma characteristics within an ECR ion source with a rectangular waveguide

To cite this article: Juan YANG *et al* 2018 *Plasma Sci. Technol.* **20** 085402

View the article online for updates and enhancements.

Related content

- Three-dimensional particle-in-cell simulation of a miniature plasma source for a microwave discharge ion thruster
  Yoshinori Takao, Hiroyuki Koizumi, Kimiya Komurasaki et al.
- EEDF by Langmuir probe diagnostics
  T Lagarde, Y Arnal, A Lacoste et al.
- Microwave plasma for energetic H- ions
  A A Skovoroda and V A Zhil'tsov

This content was downloaded from IP address 210.73.19.133 on 09/07/2018 at 03:43

© 2018 Hefei Institutes of Physical Science, Chinese Academy of Sciences and IOP Publishing Printed in China and the UK

Plasma Sci. Technol. **20** (2018) 085402 (6pp) https://doi.org/10.1088/2058-6272/aabb9f

Bended probe diagnostics of the plasma characteristics within an ECR ion source with a rectangular waveguide

Juan YANG (杨涓), Yuliang FU (付瑜亮), Xianchuang LIU (刘宪闯), Haibo MENG (孟海波) and Yizhou JIN (金逸舟)

School of Astronautic, Northwestern Polytechnical University, Xi'an 710072, People's Republic of China

E-mail: yangjuan@nwpu.edu.cn

Received 30 December 2017, revised 30 March 2018
Accepted for publication 4 April 2018
Published 6 July 2018

Abstract

To reveal the argon plasma characteristics within the entire region of an electron cyclotron resonance (ECR) ion source, the plasma parameters were diagnosed using a bended Langmuir probe with the filament axis perpendicular to the diagnosing plane. Experiments indicate that, with a gas volume flow rate and incident microwave power of 4 sccm and 8.8 W, respectively, the gas was ionized to form plasma with a luminous ring. When the incident microwave power was above 27 W, the luminous ring was converted to a bright column, the dark area near its axis was narrowed, and the microwave power absorbing efficiency was increased. This indicates that there was a mode transition phenomenon in this ECR ion source when the microwave power increased. The diagnosis shows that, at an incident microwave power of 17.4 W, the diagnosed electron temperature and ion density were below 8 eV and 3×10^{17} m^{-3}, respectively, while at incident microwave power levels of 30 W and 40 W, the maximum electron temperature and ion density were above 11 eV and 6.8×10^{17} m^{-3}, respectively. Confined by magnetic mirrors, the higher density plasma region had a bow shape, which coincided with the magnetic field lines but deviated from the ECR layer.

Keywords: ECR plasma, probe diagnosing, ion thruster

(Some figures may appear in colour only in the online journal)

1. Introduction

ECR plasma has the benefit of a high degree of gas ionization and a large volume at low gas pressure, and its associated apparatus are simple with high reliability, which makes it a candidate to be the ion source of an ion thruster. Researchers have designed and tested several ECR ion thrusters in laboratories [1–4]. Up to now, two sets of ECR ion thruster with low thrust level have been successfully used on deep space detectors and have demonstrated a unique property of this type of ion thruster, i.e. its long life span and high reliability.

Currently, the ECR ion source of ECR ion thruster with low thrust has been developed as apparatus composed of a cylindrical waveguide at TE_{11} mode and a tapered resonant cavity at TE_{111} mode [5]. To improve the ion source performance, it is necessary to investigate the properties of the ECR ion source operating at different microwave transmission modes. Therefore, a new ECR ion source, composed of a rectangular waveguide and a tapered resonant cavity operating at the TE_{01} and TE_{111} mode, respectively, was developed. The parameter that estimates the microwave energy loss in waveguide is attenuation coefficient. According to [6], it has been calculated that the attenuation coefficient of rectangular waveguide at TE_{01} mode is much lower that of cylinder waveguide at TE_{11} mode. Based on this statement, better performance of the developed ECR ion source with a rectangular waveguide is expected and the relevant primary study is plasma diagnostics within this ion source to find the space distribution of the plasma parameters.

When diagnosing plasma with a Langmuir probe, the magnetic field inside the ECR ion source generally decreases the electron current collected by the probe [7] and the diagnosed electron density is lower than the actual value. In addition, the magnetic field makes the electron energy distribution function (EEDF) deviate from the Maxwellian function [7] and the diagnosed electron temperature throughout the transition region of the probe *I-V* curve will have a larger error than that of non-magnetic plasma. However, if the influence of the magnetic field is reduced to a minimal level by taking certain measures, the Langmuir probe is still a convenient tool to diagnose plasma in the ECR ion source. One measure that can be taken is to install the probe so that the probe filament axis is perpendicular to the magnetic flux line. References [8–10] have demonstrated that this type of installation can decrease the magnetic influence on the measured current to a minimal level. Further, obtaining the plasma effective electron temperature using the diagnosed EEDF via a probe can improve the accuracy of the temperature diagnosis [7]. However, the diagnosed EEDF is easily be affected by the data processing. Therefore, diagnosing the electron temperature using the transition region of the probe *I-V* curve is still an effective method in a moderate magnetic field. In this study, a Langmuir probe whose filament axis was most likely kept perpendicular to the magnetic flux lines was used. The electron temperature was deduced using the transition region of the probe *I-V* curve, however, the ion density was deduced from the ion information.

The experimental result will provide useful information for understanding the plasma properties of the ECR ion source used in an ECR ion thruster.

2. The structure of an ECR ion source with a rectangular waveguide and plasma diagnosing system

2.1. The structure of an ECR ion source with a rectangular waveguide

As shown in figure 1, the ECR ion source was composed of a rectangular waveguide operating at the TE_{10} mode, a microwave coupling probe, a double screw adaptor, a cylindrical tapered resonant cavity and a grid system. The coupling probe was connected to a coaxial cable for wave transmission. The double screw adaptor can be regulated to decrease the reflected microwave power to the minimal level. Two magnetic rings were mounted on the inside wall of the resonant cavity to generate an ECR layer, where the magnetic flux density was 0.15 T at the 4.2 GHz microwave frequency used in experiment. The grid system included a porous screen and an accelerator grid, which were insulated from each other by a 1 mm gap. To extract the ion beams, the screen grid was positively biased to approximately 1000 V and the accelerator grid was negatively biased to several hundreds of volts.

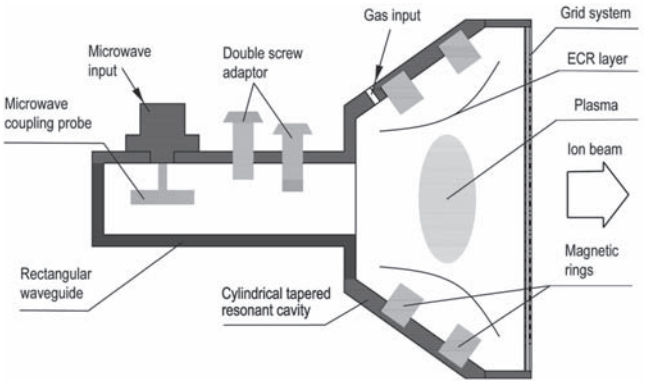

Figure 1. ECR ion source based on a rectangular waveguide.

2.2. The probe diagnosing system and method

The experimental apparatus, shown in figure 2(a), was composed of a solid-state microwave source, a circulator, an attenuator, a power metre, the ECR ion source, a Langmuir probe, a computer, a gas tank and controller, a vacuum chamber and oil diffusion vacuum pump. The microwave power incident to the ion source was calibrated before the experiment [5], and the reflected microwave power from the ECR ion source was transmitted to the power meter to be measured. As opposed to a normal ion source for ion beam extracting, only one punched screen grid for passing probe was used to diagnose the plasma, as shown in figure 2(b). The Langmuir probe moved step-by-step in the radial and axial directions.

As figure 3 shows, the Langmuir probe was composed of a ceramic tube and a tungsten filament. Inside the ECR ion source, the cyclotron radii of electron and ion, r_e and r_i, were estimated to be 0.25 mm and 2.2 mm, respectively. Compared to the probe radius $r_a = 0.1$ mm, $r_e < r_a < r_i$. Therefore, the magnetic field will change the electron saturation current, however, hardly influence the ion saturation current, hence the ion density diagnosis can be more accurate.

As figure 3 shows, for the un-bended filament, the probe axis was on the diagnosing plane and along the *x*-direction. The magnetic field components on the probe were B_x, B_y and B_z, of which the first and the latter two was parallel and vertical to the filament axis, respectively. Therefore, the influence of the magnetic field on the probe current was only from B_x [8, 9]. Similarly, for the bended filament, the influence of the magnetic field on the probe current was only from B_z. Shown in figure 4, the calculated B_x and B_z distributions [11, 12] on the diagnosing plane demonstrated that B_z was on a lower level compared to B_x. Therefore, the bended filament installation can improve the precision of the probe diagnosis.

Normally the *I-V* curve of a Langmuir probe is divided into three regions of ion saturation, transition and electron saturation. With proper plasma parameters, the thickness of the plasma sheath on the probe surface is nearly unchanged as

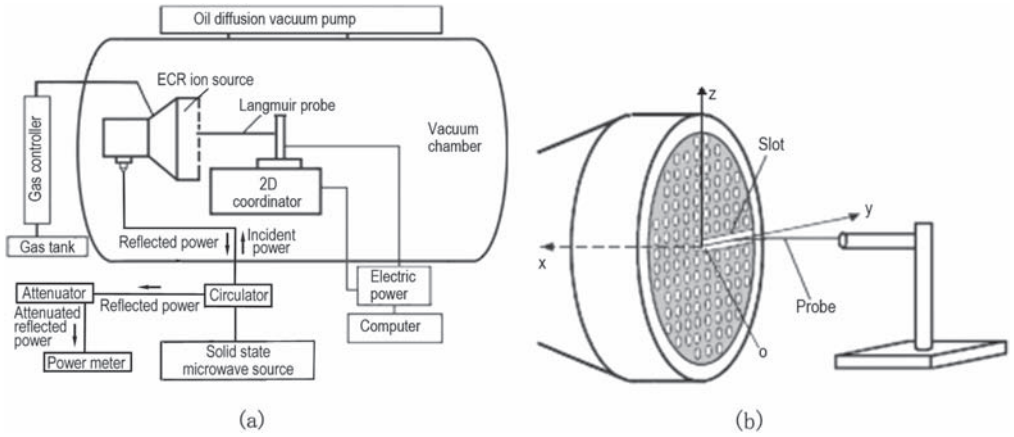

Figure 2. Experimental system for the ECR ion source: (a) experimental facility and (b) coordinate system.

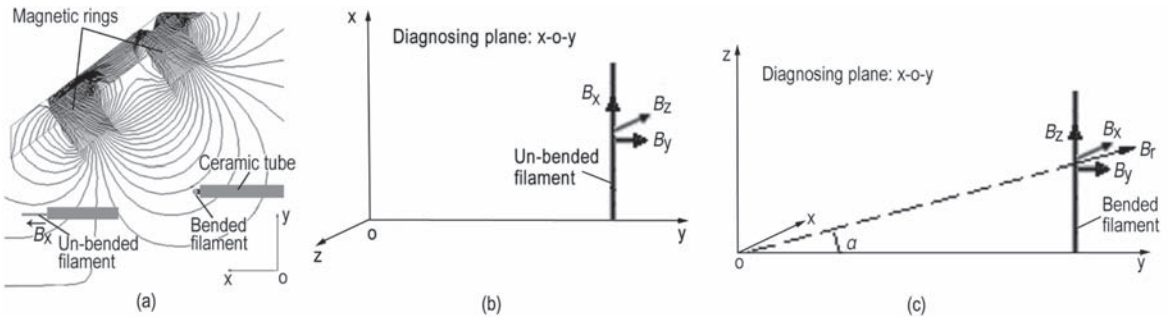

Figure 3. Probe orientation: (a) filament installation, (b) filament axis parallel to the diagnosing plane and (c) filament axis vertical to the diagnosing plane.

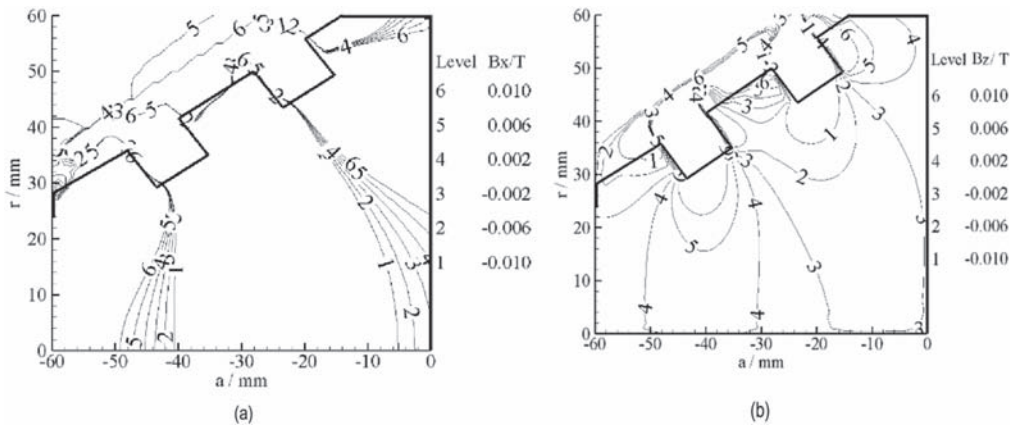

Figure 4. Magnetic flux density on the diagnosing plane: (a) B_x and (b) B_z.

the probe potential increasing and then the electron current in the saturation region saturates, as shown by the dotted line in figure 5. However, under unsuitable conditions, the electron current increases or decreases with the probe potential variation, as shown by the solid line in figure 5, which makes it difficult to find the knee point at the plasma potential. Using the second derivative variation of the *I-V* curve to judge the probe current and the potential at $\mathrm{d}^2I/\mathrm{d}V^2 = 0$ is a convenient method to determine the knee point and the plasma potential [13]. Then, the electron temperature can be deduced by

$$kT_\mathrm{e} \approx \left| \frac{d(eV)}{\mathrm{d}(\ln I_\mathrm{t})} \right|.$$

According to the orbital motion limited (OML) modal, the ion density can be obtained by

$$n_\mathrm{i} = \frac{\pi^2}{2A_\mathrm{P}^2 e^2} \frac{M}{|e|} \frac{\mathrm{d}I_i^2}{\mathrm{d}|V|}$$

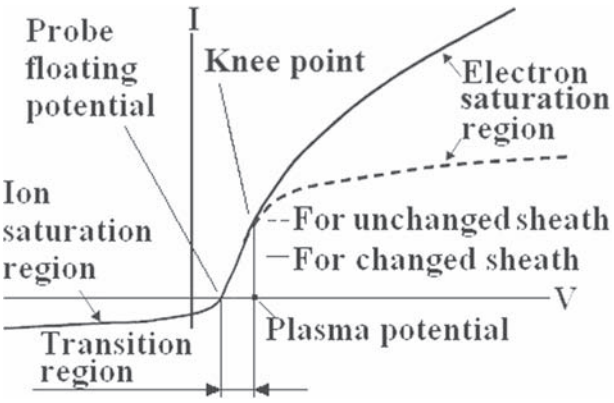

Figure 5. The *I-V* curve of a Langmuir probe.

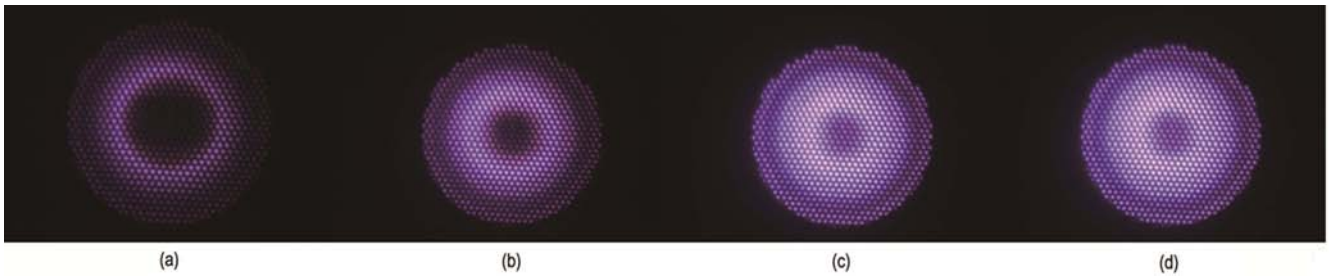

Figure 6. ECR plasma configuration at a gas volume flow rate of 4 sccm and an incident microwave power of (a) 8.8 W, (b) 17.4 W, (c) 30 W and (d) 40 W.

where k, e, I_t, I_i and A_p are Boltzmann constant, electric quantity of an electron, the collected current at the transition region, the collected current at the ion saturation region and the surface area of the probe, respectively.

3. Experimental results and discussion

Argon gas was used to operate the ECR ion source. The operation parameters were the microwave frequency at 4.2 GHz, the incident microwave power ranging from 0 W to 40 W, a gas volume flow rate of 4 sccm and the ultimate vacuum degree maintained at less than 9×10^{-4} Pa.

3.1. The configuration of the gas discharge within the ECR ion source

When the incident microwave power was gradually increased to 8.8 W, the gas ionized to form plasma with luminous ring as shown in figure 6(a). When the incident microwave power was increased to a higher level, the luminous ring would be converted into bright column with narrow central dark zone as shown in figures 6(a), (c) and (d). Figure 7 shows the curve of the microwave power absorbing efficiency, η, defined by the ratio of the ion source absorbed and the incident microwave power. The ion source absorbed microwave power is the difference between the incident and reflected microwave power. Figure 7 demonstrates that η is lower when the incident microwave power is lower than 26 W; this state can be defined as the lower mode. When the incident power is above 26 W, η is higher; this state can be defined as the higher mode. As shown in figure 6, the luminous ring at the higher mode is brighter and the dark area near the axis is narrowed compared to that at the lower mode.

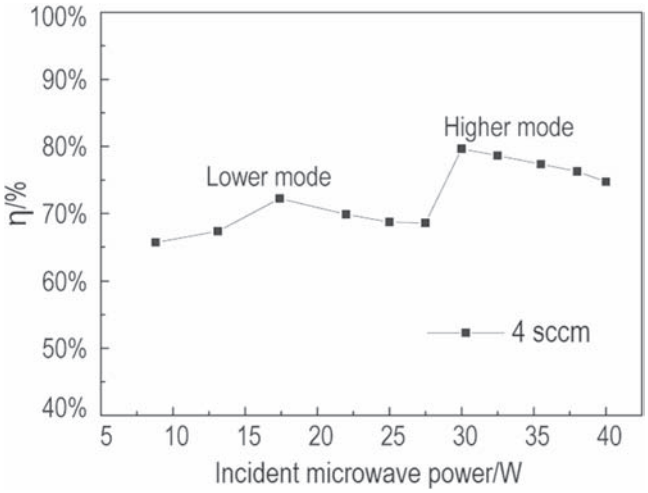

Figure 7. Microwave power absorbing efficiency versus incident microwave power.

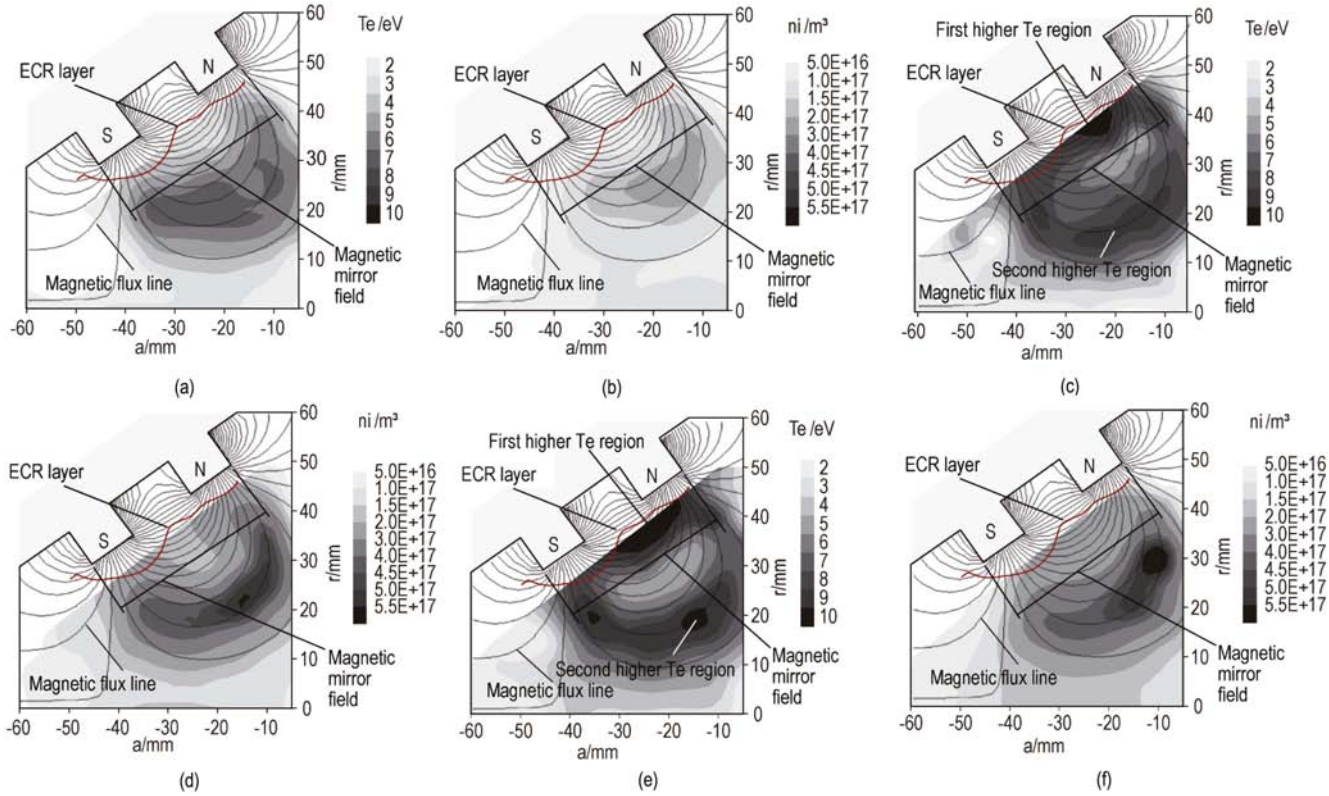

Figure 8. Diagnostic results at an Ar volume flow rate of 4 sccm: (a) T_e at 17.4 W, (b) n_i at 17.4 W, (c) T_e at 30 W, (d) n_i at 30 W, (e) T_e at 40 W and (f) n_i at 40 W.

3.2. Results and analysis of the diagnosis

The electron temperature, T_e, and ion density, n_i, at different power levels with a fixed Ar volume flow rate of 4 sccm were diagnosed as shown in figure 8, where the calculated magnetic flux lines and the ECR layer are also presented [14]. It can be seen that the ECR layer was near the sidewall of the cavity and the magnetic flux intensity sharply decayed away from the side wall. In addition, at each power level, the high T_e and n_i regions were positioned between the two magnetic rings and the high n_i region deviated from the ECR layer. As shown in figures 8(a) and (b), for the lower mode and the incident power of 17.4 W, the high-level region for T_e and n_i was exclusive and positioned between the ECR layer and the axis line. At the higher mode with an incident power of 30 W and 40 W, the high-level region for n_i was exclusive, as shown in figures 8(d) and (f). However, the high T_e region was separated into two parts, one positioned around the ECR layer and the other near the high n_i region, as shown in figures 8(c) and (e).

The T_e distribution properties in figures 8(a), (c) and (e) can be explained according to the electron heating procedure. In the ion source, electron was heated to high temperature via the ECR procedure occurred near the ECR layer because this resonating condition was only associated with the magnetic field. Further, electron was also heated to higher temperature via the high hybrid wave resonance procedure in the region of lower magnetic flux intensity and higher plasma density as soon as the resonating condition was satisfied. Therefore, it is reasonable that at the higher mode, the high T_e region separated into two parts, one near the ECR layer and the other in the low magnetic flux intensity region. At the lower mode, however, the region of high T_e could be only observed at the low magnetic flux intensity region because the strong magnetic field at ECR layer generated strong interference on the measurement of very weak probe current, and hence accurate T_e diagnosing result at ECR layer could not be obtained.

The n_i distribution property can be explained according to the electron movement in the magnetic mirror field formed by the two magnetic rings shown in figures 8(b), (d) and (f). With the confining magnetic mirror, the electrons inside the ion source were restricted around the magnetic flux lines and drifted to the low B region due to the electron momentum and magnetic torque conservation and the effect of diffusion [7]. Therefore, the electrons would gather in the region of low magnetic field intensity, and hence the high electron density region was in a bow shape coinciding with the magnetic field lines. According to the bipolar diffusion property of plasma, the ion density distribution would be similar to that of the electrons. Therefore, the high n_i region corresponded to that of the low magnetic field intensity and showed a bow shape coinciding with the magnetic field lines.

It is a fact that dense electrons cause frequent collisions with heavy particles and increase the density of the excited heavy particles. When the dense excited heavy particles spontaneously decayed to the de-excited state, the stronger emission line was observed, which generated to a bright

plasma image [15]. Therefore, it is reasonable that the diagnosed high n_i region corresponded to the ring shape of the plasma, as shown in figure 4. With the power increasing, the ion and electron density increased and plasma diffused from the high-density area to the axis line, which caused the centre dark area of the ion source to be narrowed.

4. Conclusions

To study the plasma characteristics within an ECR ion source with a rectangular waveguide, a detailed diagnosis of the distribution of the plasma parameters was completed. In the experiment, a Langmuir probe with a filament perpendicular to the diagnosing plane was used. The experiment results were as follows.

(1) The lower and higher modes of the ECR ion source were identified. At the lower mode, the ion source operated at lower power and efficiency and the electron temperature and ion density were lower. At the higher mode, the electron temperature and the ion density were higher.
(2) At an incident microwave power of 17.4 W, the diagnosed electron temperature and ion density were below 8 eV and $3 \times 10^{17}\,\mathrm{m}^{-3}$, respectively. While at an incident microwave power of 30 W and 40 W, the maximum electron temperature and the ion density were above 11 eV and $6.8 \times 10^{17}\,\mathrm{m}^{-3}$, respectively.
(3) In the ion source, electrons received microwave energy according to the ECR and the high hybrid wave resonance procedure, which caused the high electron temperature region separated into two parts: one around the ECR layer and the other in lower magnetic flux intensity region.
(4) Due to the confining magnetic mirror and plasma transport property, the high n_i region positioned in the low magnetic field intensity area and showed a bow shape coinciding with the magnetic field lines. The diagnosed electron temperature and ion density distributions corresponded to the actual plasma image. When the ion source state changed from the lower to higher mode, the high n_i and plasma luminance region increased.

Acknowledgments

The authors acknowledge the financial support of National Natural Science Foundation of China (Grant No. 11475137).

References

[1] Koizumi H and Kuninaka H 2010 *J. Propuls. Power* **26** 601
[2] Funaki I *et al* 2006 *IEEE Trans. Plasma Sci.* **34** 2031
[3] Funaki I, Kuninaka H and Toki K 2004 *J. Propuls. Power* **20** 718
[4] Goede H 1987 *J. Spacer. Rockets* **24** 437
[5] Jin Y Z *et al* 2016 *Acta Phys. Sin.* **65** 045201 (in Chinese)
[6] Ying J N 2007 *Microwave and Photoconductive Wave Technology* (Beijing: National Defend Industry Press)) (in Chinese)
[7] Ma T C, Hu X W and Chen Y H 2012 *Principles of Plasma Physics* (Hefei: University of Science and Technology of China Press) (in Chinese)
[8] Shikama T, Kitaoka H and Hasuo M 2014 *Phys. Plasmas* **21** 073510
[9] Demidov V I, Ratynskaia S V and Rypdal K 1999 *Rev. Sci. Instrum.* **70** 4266
[10] Demidov V I *et al* 2002 *Rev. Sci. Instrum.* **73** 3409
[11] Jin Y Z *et al* 2016 *Plasma Sci. Technol.* **18** 744
[12] Yang T L *et al* 2009 *Chin. Space Sci. Technol.* **29** 46 (in Chinese)
[13] Lieberman M A and Lichtenberg A J 2005 *Principles of Plasma Discharges and Materials Processing* 2nd edn (New York: Wiley)
[14] Feng B B *et al* 2016 *J. Propuls. Technol.* **09** 1794 (in Chinese)
[15] Yang J *et al* 2013 *Phys. Plasmas* **20** 123505